

Errors Estimation for Evaluating Mixed-Mode Stress Intensity Factors for Cracks Emanating from Sharp Notches Using Simulated Photoelasticity

M.H. Ghasemi, M. Khaleghian and N. Soltani

School of Mechanical Engineering, Tehran University, Tehran, Iran

Abstract: In this paper, errors involved in extracting stress intensity factors from photoelastic fringe pattern, which were simulated for crack estimated. The estimated errors do not contain the errors associated with the optical apparatus, but only consist of the errors associated with discretization and extraction of data for SIF's calculation to accomplish that. A series of fringe pattern were simulated for specimens containing various cracks in finite strips under remote tensile loading. In addition, by combination of fracture mechanics and photoelasticity's equations and digital image analysis an algorithm is developed for determining stress intensity factors (SIFs). In addition, to utilize the advantage of "whole-field" photoelasticity and to minimize the random experimental errors, the over deterministic least-squares method of Sanford combined with Newton-Raphson method is used to obtain SIFs.

Key words: Stress Intensity Factors(SIFs) • Photoelastic Fringe • Least-Square Method • Newton-Raphson

INTRODUCTION

There are numerous applications of optical stress analysis methods where in the objective of the experiment is to compare a theoretical solution with the experimental result. Photoelasticity is a useful technique for stress analysis, which requires the processing of fringe patterns. The basic instrument in photoelasticity is the so-called polariscope. It has been used extensively for the study of various static and dynamic fracture problems.

One of the most attractive qualities of photoelasticity is that it provides a simple method for direct examination of the whole-field stress distribution. Reviews of techniques, which have been developed since 1979, have periodically been published in journals [1-3] and in a book dedicated to automated photoelasticity [4]. One which is of particular interest today, is the determination of the fracture-mechanics geometric parameter(s), i.e., the stress intensity factor(s), for a specific geometry from the characteristic features of the fringe loops in the neighborhood of the crack tip.

Starting from first applications, such as fringe thinning methods [5] and half fringe photoelasticity [6], a variety of more advanced techniques has been developed. In particular, methods in white light, based on spectral content analysis (SCA) [7-10] and RGB photoelasticity [11-14], phase stepping methods [15-22] and Fourier

transform methods (FTMs) [23-26] have significantly contributed to automation of procedures to acquire and process photoelastic data.

The analysis of the photoelastic images has traditionally been time-consuming and observer dependent, but in recent years computer image processing has been applied to the photoelastic stress analysis to automate determination of the stress field. In any automated algorithm for interpreting photoelastic fringe patterns, it is necessary to understand and quantify sources of error in the measurement system. Automated photoelasticity is influenced both by the usual sources of errors common to the methods of digital image processing and by the typical sources of errors of photoelasticity (see [4], p. 172 and [27, 28]).

Currently, most investigators solve both of these types of errors with point-matching techniques. No advantage is taken of the fact that the fringe pattern, by its very nature, contains an unlimited number of data points.

Once that is done, suitable algorithms that can handle the inherent noise in the signal can be constructed. There will usually be trade-offs in the algorithm among those that work best in ideal situations versus those that function robustly on actual photoelastic data. Errors in automated measurements consist of two main types: those associated with the optical apparatus and those

associated with the sensor. Some of the errors associated with the optical arrangement are also present when making manual measurements; e.g., the planes of the optical path and the angular orientation of the elements should be precisely set. Optical errors include linear and angular alignment, quarter-wave plate mismatch, material in homogeneities and spatial and temporal variations of light. Sensor errors include discretization of intensity data, spatial quantization and geometric distortion. The sources of errors inherent in the photoelastic coatings themselves have received less attention in the literature.

However, with the emergence of computers and image processing techniques becoming a reality in optical stress analysis (e.g., Ref. 2), the full potential of whole-field fringe-pattern analysis methods can be more readily utilized. What are needed now are computer-based algorithms to take advantage of these technologies.

The purpose of this paper investigation is to develop an algorithm for determining Mode I and II stress intensity factors by using Williams' [29] stress equations in combination with the method of photoelasticity and digital image processing. To utilize the advantage of "whole-field" photoelasticity and minimize random experimental errors in measurements of r and θ , the over deterministic least squares method of Sanford [30] combined with Newton-Raphson iterative method was used to solve for K_I and K_{II} from a nonlinear relationship.

The Method of Photoelasticity: Photoelasticity is an experimental method to determine stress distribution in a material. The method is mostly used in cases where mathematical methods become quite cumbersome. Unlike the analytical methods of stress determination, photoelasticity gives a fairly accurate picture of stress distribution even around abrupt discontinuities in a material. The method of photoelasticity has been used extensively in the past for investigating elastic stresses in cracked specimens. The method serves as an important tool for determining the critical stress points in a material and is often used for determining stress concentration factors in irregular geometries.

According to the classical concepts of photoelasticity, the mathematical equation for an isochromatic fringe is written generally as:

$$2(\sigma_1 - \sigma_2) = \frac{Nf}{h} \quad (1)$$

Where $(\sigma_1 - \sigma_2)$ is the maximum in-plane shear stress; N ; the fringe order; h ; the specimen thickness; f is the material fringe value. The elastic stresses near the tip of a

mixed mode crack embedded in a homogeneous and isotropic material can be written as:

$$\sigma_{xx} = \frac{K_I}{\sqrt{2\pi r}} \cos \frac{\theta}{2} \left[1 - \sin \frac{\theta}{2} - \sin \frac{3\theta}{2} \right] - \frac{K_{II}}{\sqrt{2\pi r}} \sin \frac{\theta}{2} \left[2 + \cos \frac{\theta}{2} \cos \frac{3\theta}{2} \right] \quad (2)$$

$$\sigma_{yy} = \frac{K_I}{\sqrt{2\pi r}} \cos \frac{\theta}{2} \left[1 - \sin \frac{\theta}{2} \sin \frac{3\theta}{2} \right] + \frac{K_{II}}{\sqrt{2\pi r}} \sin \frac{\theta}{2} \cos \frac{\theta}{2} \cos \frac{3\theta}{2} \quad (3)$$

$$\tau_{xy} = \frac{K_I}{\sqrt{2\pi r}} \sin \frac{\theta}{2} \cos \frac{\theta}{2} \cos \frac{3\theta}{2} + \frac{K_{II}}{\sqrt{2\pi r}} \cos \frac{\theta}{2} \left[1 - \sin \frac{\theta}{2} \sin \frac{3\theta}{2} \right] \quad (4)$$

Where r and θ are the in-plane polar coordinates centered at the crack tip and K_I is the mode I stress intensity factor and K_{II} is the mode II stress intensity factor.

As we know the relation between the maximum shear stress (τ_m) and stress components (σ_{xx}), (σ_{yy}) and (τ_{xy}) can be shown as:

$$(2\tau_m)^2 = (\sigma_{xx} - \sigma_{yy})^2 + 4\tau_{xy}^2 \quad (5)$$

By replacing Eqs. (1)-(4) in Eq. (5) the fringe pattern developing near a crack can be shown mathematically as:

$$\tau_{\max} = \frac{Nf}{2h} = \frac{1}{2(2\pi r)^{0.5}} \{ [K_I \sin \theta + 2K_{II} \cos \theta]^2 + [K_{II} \sin \theta]^2 \}^{1/2} \quad (6)$$

With knowing N for only 2 points at the stress field, we can obtain K_I and K_{II} from Eq. (6).

Problem Definition: The geometrical configuration is depicted in Fig. 1. the length of crack is c and length of root of notch is shown by a . In addition a finite element model of the specific geometry is constructed (Fig. 2), then it is analyzed with some popular FEM softwares. According to this approach the results, which are shown in Fig. 1 and Fig. 2:

Numerical Analysis: To solve for the unknown stress intensity factors, K_I and K_{II} in Eqs. (2)-(4), the over deterministic least squares algorithm of Sanford (e.g., Ref. 30) in conjunction with Newton-Raphson iterative method is used. This technique of using more data than the two needed to solve for the two unknowns takes advantage of whole-field photoelastic data and reduces the experimental error. From photoelasticity the maximum in-plane shear stress can be expressed as Eq. (1).

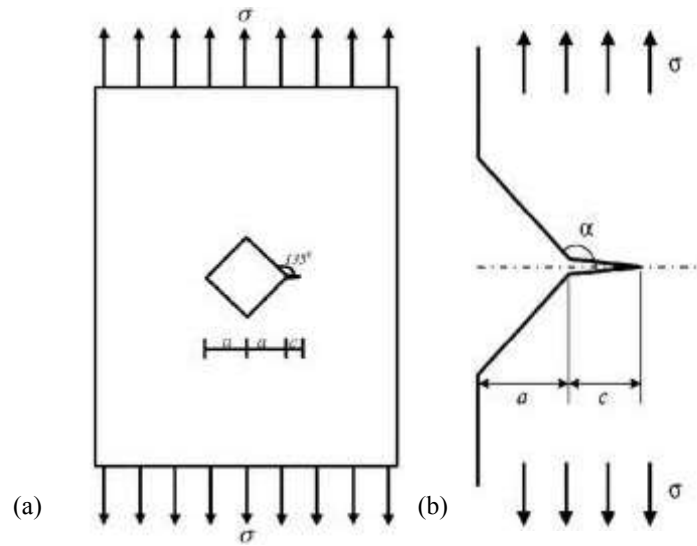


Fig. 1: The model of sharp notch, which is used in this paper

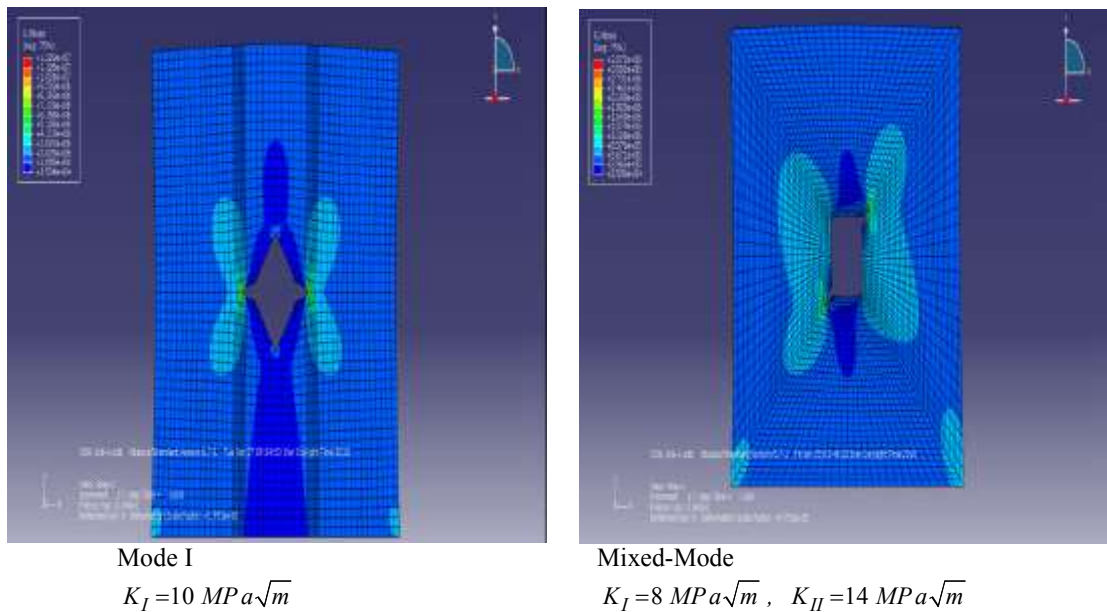


Fig. 2: A Finite Element Model of specific geometry stress contours at the vicinity of the crack

According to Eq. (6) to establish the relationship between N and the stress intensity factors, the maximum in-plane shear stress is written in terms of polar stresses, i.e. Define a function G such that:

$$G(K_I, K_{II}) = (\sigma_r - \sigma_\theta)^2 + 4(\tau_{r\theta})^2 - \left(\frac{Nf}{h}\right)^2 \quad (8)$$

After substitution of stresses from Eqs. (2)-(4), a truncated Taylor series expansion about the unknown parameters, K_I and K_{II} , will result in a lineared equation in the form of

$$(G_k)_{i+1} = (G_k)_i + \left(\frac{\partial G_k}{\partial K_I}\right)_i \Delta K_I + \left(\frac{\partial G_k}{\partial K_{II}}\right)_i \Delta K_{II} \quad (9)$$

Where subscript I denote the iteration step. From eq. (9), if estimates of K_I and K_{II} , combined with photoelastic data (r , θ and N) are given, one can obtain the corrections ΔK_I and ΔK_{II} , to those estimates. The corrections are added to the estimates and new estimates of K_I and K_{II} are obtained. This procedure is repeated until the desired result, $(G_k)_{i+1} = 0$ is obtained. The detailed steps are given in ref. [31].

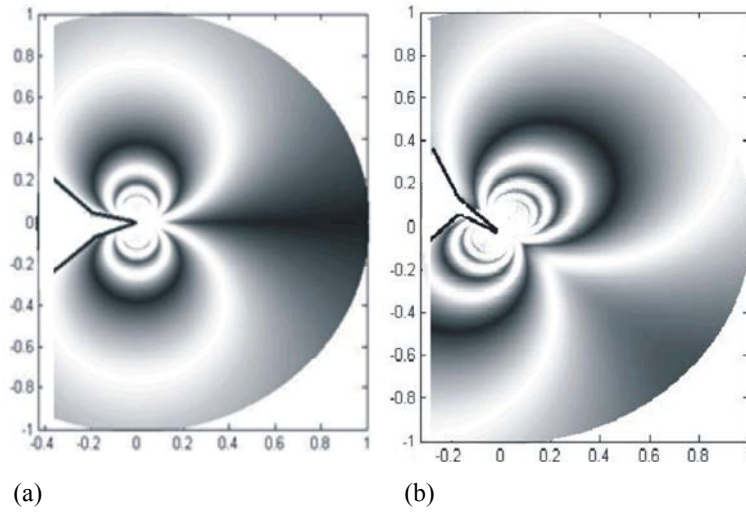


Fig. 3: Simulated photoelastic fringes

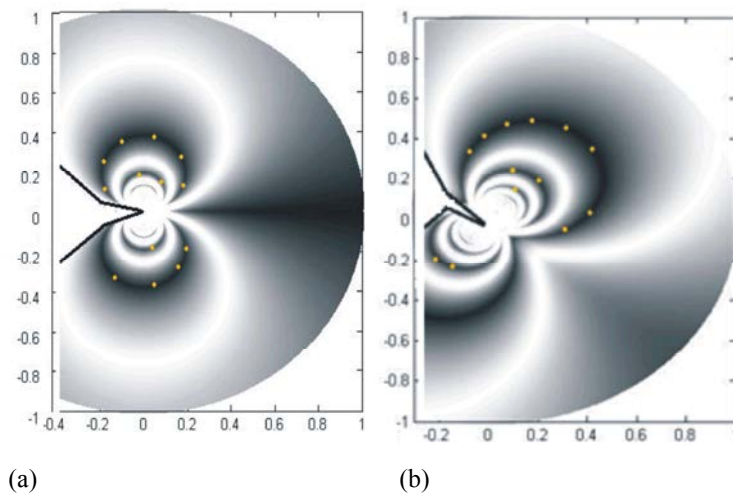


Fig. 4: Selected points for SIFs determination

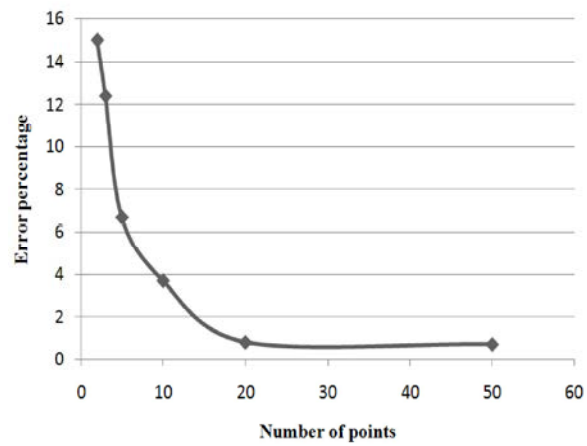


Fig. 5: Error analysis for photoelastic fringes

DISCUSSION

Having K_I and K_{II} and using Eqs. (1)-(5), approximation of photoelasticity fringe pattern would be depicted theoretically. A computer code was written in order to simulate the photoelastic fringes (Fig. 3)

Moreover, with using an inverse method and image processing techniques, finding SIFs for all photoelastic images would be possible. In this method to determine SIFs, Having the Point coordinates and using fracture and photoelasticity equations are needed. Also more than 2 points can be selected and using least-square method and solving over determined Equations to determine the SIFs. Because of photoelastic image inaccuracy and elusion in accurate round fringe point the determination of K_I and K_{II} contains error. The average values of SIFs obtained from the photoelastic fringe patterns at different images levels were calculated. Fig. 5 shows the average value of K_I and K_{II} for 2, 3, 5, 10, 20 and 50 points and the error of SIFs for each of them. Fig. 4 is shown the points which are selected to obtain SIFs. Also Fig. 5 depicts the error percentage to selected points.

CONCLUSION

In conclusion, the simulation of photoelastic fringes to and also finding SIFs by this inverse method can improve this method and decrease the errors. Also Determination of SIFs for some cracks has shown that with increasing the selecting point to 20 the error would decrease and after 20 points the range of error isn't variable. For this, selecting 20 points is logical to optimize the K_I and K_{II} .

REFERENCES

1. Patterson, E.A., W. Ji and Z.F. Wang, 1997. On image analysis for birefringence measurements in photoelasticity. *Opt Lasers Eng.*, 28(1): 17-36.
2. Ramesh, K. And S.K. Mangal, 1998. Data acquisition techniques in digital photoelasticity: a review. *Opt Lasers Eng.*, 30(1): 53-75.
3. Ajovalasit, A., S. Barone and G. Petrucci, 1998. A review of automated methods for the collection and analysis of photoelastic data. *J. Strain Anal.*, 33(2): 75-91.
4. Ramesh, K., 2000. *Digital photoelasticity*. Berlin: Springer.
5. Muller, R.K. and L.R. Saackel, 1979. Complete automatic analysis of photoelastic fringes. *Exp. Mech.*, 19(7): 245-51.
6. Voloshin, A.S. and C.P. Burger, 1983. Half fringe photoelasticity: a new approach to whole-field stress analysis. *Exp. Mech.*, 23(3): 304-13.
7. Redner, A.S., 1985. Photoelastic measurements by means of computer-assisted spectral contents analysis. *Exp. Mech.*, 25(2): 148-53.
8. Sanford, R.J. and V. Iyengar, 1985. The measurement of the complete photoelastic fringe order using a spectral scanner. *Proceeding of the SEM Conference on Experimental Mechanics*, Las Vegas, pp: 160-8.
9. Sanford, R.J., 1986. On the range of accuracy of spectrally scanned white light photoelasticity. *Proceeding of the SEM Conference on Experimental Mechanics*, New Orleans, pp: 901-8.
10. Voloshin, A.S. and A.S. Redner, 1989. Automated measurement of birefringence: development and experimental evaluation of the techniques. *Exp. Mech.*, 29(3): 252-7.
11. Ajovalasit, A. And G. Petrucci, 1990. Automatic analysis of photoelastic fringes in white light. *Proceedings of the XVIII AIAS Conference*, Istituto di Ingegneria Meccanica, Universit'a di Salerno, pp: 395-407 (in Italian).
12. Ajovalasit, A., S. Barone and G. Petrucci, 1995. Automated photoelasticity in white light: influence of quarter wave plates. *J. Strain Anal.*, 30(1): 29-34.
13. Ajovalasit, A., S. Barone and G. Petrucci, 1995. Toward RGB photoelasticity Full field photoelasticity in white light. *Exp. Mech.*, 35(3): 193-200.
14. Ramesh, K. And S.S. Deshmukh, 1996. Three fringe photoelasticity Fuse of colour image processing hardware to automate ordering of isochromatics. *Strain*, 32(3): 79-86.
15. Hecker, F.W. and B. Morche, 1986. Computer-aided measurement of relative retardations in plane photoelasticity. In: Wieringa H, editor. *Experimental stress analysis*. Dordrecht: Martinus Nijhoff Publ., pp: 535-42.
16. Patterson, E.A. and Z.F. Wang, 1991. Towards full field automated photoelastic analysis of complex components. *Strain*, 27(2): 49-56.
17. Carazo-Alvarez, J., S.J. Haake and E.A. Patterson, 1994. Completely automated photoelastic fringe analysis. *Opt Lasers Eng.*, 21(3): 133-49.

18. Mawatari, S., M. Takashi, Y. Toyada and T.A. Kunio, 1990. single valued representative function for determination of principal stress direction in photoelastic analysis. Proceedings of the Ninth International Conference on Experimental Mechanics, vol. 5, Copenhagen, pp: 2069-78.
19. Petrucci, G., 1997. Full field automatic evaluation of isoclinic parameter in white light. *Exp. Mech.*, 37(4): 420-6.
20. Buckberry, C. And D. Towers, 1996. New approaches to the full-field analysis of photoelastic stress patterns. *Opt. Lasers Eng.*, 24(516): 415-28.
21. Lesniak, J.R. and M.J. Zickel, 1998. Application of automated grey-field polariscope. Proceedings of the SEM Spring Conference on Experimental and Applied Mechanics, Houston, pp: 298-301.
22. Patterson, E.A. and Z.F. Wang, 1998. Simultaneous observation of phase-stepped images for automated photoelasticity. *J. Strain Anal.*, 33(1):1-15 (Erratum: *J. Strain Anal.*, 33(5): 400).
23. Quan, C., P.J. Bryanstone-Cross and T.R. Judge, 1993. Photoelasticity stress analysis using carrier fringe and FFT techniques. *Opt Lasers Eng.*, 18(2): 79-108.
24. Morimoto, Y., Y. Morimoto and T. Hayashi, 1994. Separation of isochromatics and isoclinis using Fourier transform. *Exp. Tech.*, 18(5): 13-7.
25. Ng, T.W., 1997. Photoelastic stress analysis using an object step-loading method. *Exp. Mech.*, 37(2): 137-41.
26. Zuccarello, B., 1998. A newautom ated method for the analysis of isochromatics in photoelasticity. Proceedings of the XXVII AIAS National Conference, Perugia, pp: 1165-74 (in Italian).
27. Patterson, E.A., W. Ji and Z.F. Wang, 1997. On image analysis for birefringence measurements in photoelasticity. *Opt Lasers Eng.*, 28(1): 17-36.
28. Haake, S.J., Z.F. Wang and E.A. Patterson, 1993. Evaluation of full field automated photoelastic analysis based on phase stepping. *Exp Tech.*, 17(6): 19-25.
29. Williams, M.L., 1952. Stress singularities resulting from various boundary conditions in angular corners of plates in extension. *Trans. ASME, J. Appl. Mech.*, 19: 526-528.
30. Sanford, R.J., 1980. Application of the least squares method to the photoelastic analysis. *Exp. Mech.*, 20(6): 192-197.
31. Mahinfalah, M., 1988. Photoelastic determination of stress intensity factors for reentrant corners. PhD Thesis, Iowa State University, Ames, Iowa.